Distinct in-plane resistivity anisotropy in a detwinned FeTe single crystal: Evidence for a Hund's metal

Juan Jiang (姜娟), C. He (贺诚), Y. Zhang (张焱), M. Xu (徐敏), Q. Q. Ge (葛青亲), Z. R. Ye (叶子荣), F. Chen (陈飞), B. P. Xie (谢斌平),* and D. L. Feng (封东来)†

State Key Laboratory of Surface Physics, Department of Physics, and Advanced Materials Laboratory, Fudan University, Shanghai 200433, People's Republic of China

(Received 29 June 2013; revised manuscript received 31 August 2013; published 17 September 2013)

The in-plane resistivity anisotropy has been studied with the Montgomery method on the detwinned parent compound of the iron-based superconductor FeTe. The observed resistivity in the antiferromagnetic (AFM) direction is larger than that in the ferromagnetic (FM) direction, which is different from that observed in $BaFe_2As_2$ before. We show that the opposite resistivity anisotropy behavior in FeTe could be attributed to the strong Hund's rule coupling effects, which should be understood in a localized picture: Hund's rule coupling makes hopping along the FM direction easier than along the AFM direction in FeTe, similar to the colossal magnetoresistance observed in some manganites.

DOI: 10.1103/PhysRevB.88.115130 PACS number(s): 74.25.F−, 74.70.Xa, 72.15.−v, 75.30.Fv

I. INTRODUCTION

Most unconventional superconductors are in the vicinity of certain magnetically ordered states. For cuprates, the antiferromagnetic Mott insulator parental state is suggested to be intimately related to the superconducting mechanism. For iron-based high-temperature superconductors (Fe-HTS), several types of antiferromagnetic parental states have been discovered, including the collinear antiferromagnetic state (CAF) in iron pnictides,[1–4] the bicollinear antiferromagnetic state (BCAF) in FeTe [see Fig. 1(a)],[5] the insulating block-antiferromagnetic state of $K_2Fe_4Se_5$, and a semiconducting collinear antiferromagnetic state in vacancy-ordered $K_xFe_{1.5}Se_2$.[6,7]

The CAF state breaks the fourfold symmetry, entering a nematic or twofold symmetric phase, and it was suggested to drive the tetragonal-to-orthorhombic structural transition, as illustrated in Fig. 1(a).[8,9] There are usually twinned domains in the orthorhombic states, but it has been shown that the twinning could be removed with a uniaxial pressure.[10] In detwinned $BaFe_{2-x}Co_xAs_2$, the resistivity in the antiferromagnetic (AFM; a_O) direction is found to be significantly smaller than that in the ferromagnetic (FM; b_O) direction.[10] Such a resistivity anisotropy could be taken as a hallmark of the nematic phase. In addition, a magnetic torque experiment in $BaFe_2As_{2-x}P_x$ presents strong evidence that nematicity is an intrinsic property.[11] Later, the resistivity anisotropy was shown to be much reduced for the postannealed $BaFe_{2-x}Co_xAs_2$,[12] and recent systematic measurements argue that the anisotropic resistivity is caused by anisotropic scattering of Co dopants.[13] Furthermore, the resistivity anisotropy was found to be much weaker in detwinned $Ba_{1-x}K_xFe_2As_2$ (Ref. 14) and even to be reversed at higher potassium concentrations.[15] Whether the resistivity anisotropy is an intrinsic property or not is still under debate. Theoretically, some suggest that it is an indication of the presence of orbital ordering,[16] while others suggest that the details of the quasiparticle scattering and Fermi-surface topology might be responsible for the diversified behaviors in the electron- and hole-doped $BaFe_2As_2$.[17]

Previous studies were focused on the so-called 122, 111, and 1111 series of pnictide Fe-HTS;[10–14,18–20] we here report the temperature dependence of resistivity anisotropy in 11 series of chalcogenide Fe-HTS, specifically, in FeTe single crystals detwinned with uniaxial strain. Both as-grown samples and annealed samples with higher quality are studied. The anisotropy is reduced in the annealed sample, as expected. But, intriguingly, the resistivity anisotropy observed exhibits the opposite behavior to that of the 122 series. That is, the resistivity along the AFM direction is larger than that along the FM direction. Although we still cannot exclude the influences of impurity scattering as reported elsewhere,[13] the dramatic difference in the resistivity anisotropy behavior of FeTe is most likely caused by Hund's rule coupling between the large localized moment $\vec{S}$ and the spin of the itinerant electrons $\vec{s}$. The exchange interaction term $J_H\vec{S}\cdot\vec{s}$ (with J_H being the Hund's rule coupling constant) induces an extra potential barrier for the electrons to hop in the AFM direction, and thus the resistance is higher in the AFM direction than in the FM direction. This is analogous to the hopping facilitated by the ferromagnetic spin orientation in the colossal magnetoresistance (CMR) effect of certain manganites.[21] Our results suggest that while on-site Coulomb interaction U may not be strong for Fe-HTS, J_H is the dominating interaction that gives strong on-site correlations in such a multiorbital system, just like in the manganites.

II. EXPERIMENTAL RESULTS AND DISCUSSIONS

The as-grown α-FeTe single crystals were synthesized following previous reports,[8,22] and the annealed α-FeTe single crystals were achieved by annealing the as-grown samples at 800 °C in an evacuated quartz tube. As-grown and annealed samples have ∼8.8% and ∼2.3% excess Fe, respectively, based on our energy-dispersive x-ray spectroscopy (EDX) data. It has been reported before that annealing in air would more effectively reduce the interstitial iron than annealing in vacuum under temperatures no more than 400 °C.[23] It is likely that the higher temperature during our annealing process helps reduce the interstitial iron more effectively, while the origin for the change of the iron concentration needs to be further studied.

Since the single crystals naturally contain twin domains in the orthorhombic phase, we designed a detwinning device

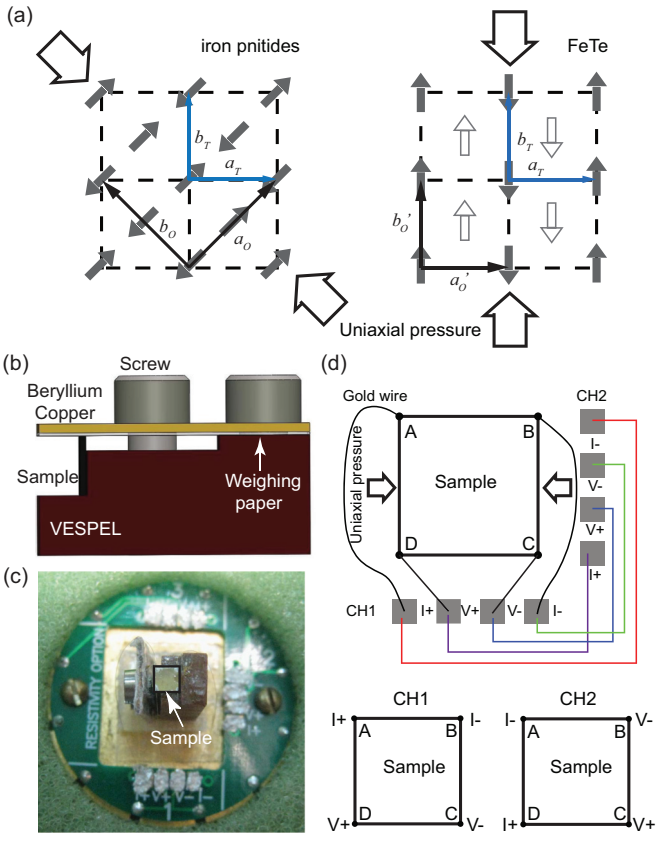

FIG. 1. (Color online) (a) The schematics of the spin structures in iron pnictides and FeTe following Refs. 26 and 5; the hollow arrows show the directions of the uniaxial pressure for detwinning. In iron pnictides, the a_O (b_O) axis is 45° to the tetragonal a_T (b_T) axis,[26] while in FeTe, the a'_O (b'_O) axis is the same as that in the tetragonal phase.[5] For both iron pnictides and FeTe, the spins are aligned antiferromagnetically along a_O/a'_O and ferromagnetically along b_O/b'_O. (b) The design of the detwinning device; a piece of weighing paper is inserted between the sample and the beryllium copper piece to ensure the insulation. (c) A detwinning device mounted on a PPMS puck. (d) The two configurations in the Montgomery method for in-plane resistivity measurement.

similar to that of Chu *et al.* [see Fig. 1(b)],[10] which puts uniaxial pressure along one of the orthorhombic directions. It has been shown that the twinning in iron pnictides could be removed effectively in this way,[24] and b_O is preferred along the pressurized direction in the orthorhombic phase since the lattice constant b_O is slightly smaller than a_O.[25] The same device has been used in $BaFe_2As_2$ and NaFeAs, where the detwinning effect has been successfully observed. As shown in Fig. 1(c), the FeTe single crystal was cut into a rectangular shape with edges along the a'_O and b'_O axes determined through its Laue x-ray diffraction pattern, and it was mounted on the detwinning device. We found that this device could effectively reduce the twinning in FeTe since b'_O is smaller than a'_O in FeTe as well. However, since low-temperature polarized light imaging and local diffraction techniques are not accessible in our case, it is hard to assess the completeness of the detwinning. Although we have applied the highest possible compressional force so that the sample would not be damaged, the detwinning could still be incomplete. However, we note that this would not influence the qualitative conclusions made based on the data.

The resistivity measurements were conducted with a Quantum Design physical property measurement system (PPMS), using the Montgomery method as shown in Fig. 1(d).[12,27,28] This method has the ability to obtain the resistances along both orthorhombic directions under the same condition, compared with the usual four-lead method.[29,30]

The resistances of as-grown and annealed FeTe single crystals are shown in Figs. 2(a) and 2(c), respectively, as a function of temperature. Both of them exhibit semiconducting behaviors in the paramagnetic state and then become metallic after a sharp drop around T_N, corresponding to the structural/BCAF transition.[31] Moreover, the hysteresis loop is observed in both the magnetic susceptibility and resistivity, with a width of about 1 K, revealing its first-order nature.[32] For the as-grown sample, when a uniaxial pressure is applied along the b'_O direction with the detwinning device, both R_a and R_b still exhibit sharp drops around 64.5 K (T_N); however, the resistivity anisotropy appears below T_A, which is about 5 K above T_N, as shown in Fig. 2(b). On the contrary, the anisotropy above T_N disappears in the annealed sample, as shown in Fig. 2(d). Furthermore, T_N in the annealed sample in Fig. 2(d) is about 65.5 K, a bit higher than that of the as-grown sample in Fig. 2(b), which might be due to different iron contents.[33] Most strikingly, we found that the anisotropies in both as-grown and annealed samples exhibit opposite behavior to that in the 122 iron-based superconductors observed before; that is, R_a in the AFM direction is larger than R_b in the FM direction for FeTe.

The FeTe single crystal exhibits a sharp resistivity jump at T_N, reflecting the strong first-order nature of the transition, which is similar to the 122 parental compound $SrFe_2As_2$.[30] Interestingly, T_A does not extend far above T_N for as-grown FeTe here and for $SrFe_2As_2$ reported elsewhere, compared with the long tails in the resistivity anisotropy of NaFeAs and $BaFe_2As_2$.[19,29,30] On the one hand, it might suggest that the nematic fluctuation is suppressed for the first-order phase transition, whereas it is rather strong above the weak first-order or second-order phase transition temperature in NaFeAs and $BaFe_2As_2$. An obvious difference between the as-grown sample and the annealed one is that the anisotropy happens at a higher temperature T_A, while in the annealed one the anisotropy has only been observed below T_N. On the other hand, it might indicate that for the first-order transition case, the anisotropy above T_N is induced by impurity scattering since the annealed FeTe possesses ~2.3% excess Fe, which is much cleaner than the as-grown one with ~8.8% excess Fe.

However, even in the clean annealed sample, the resistivity anisotropy below T_N cannot be removed. According to the data shown in Fig. 2, the resistivity anisotropy has been reduced by ~33% in the annealed sample (assuming the levels of detwinning are similar in the annealed and as-grown samples), while the excess impurity of iron has been reduced by as much as ~74%. Although we cannot exclude the possibility that the anisotropic impurity scattering effect has some influence on the resistivity anisotropy below T_N in the annealed sample, the anisotropy should not be wholly contributed by the impurity scattering, and it is most likely an intrinsic property.

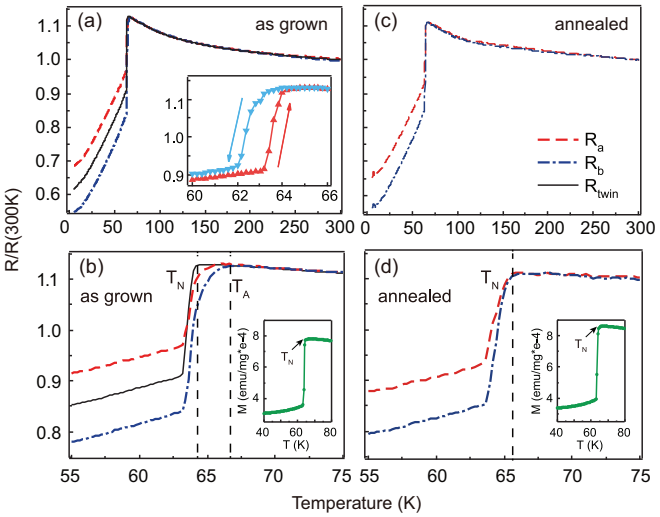

FIG. 2. (Color online) (a) Temperature dependence of the in-plane resistivity of an as-grown FeTe single crystal. The inset shows the hysteresis loop observed in the resistivity with a width of about 1 K. (b) An enlargement of (a); the inset is the magnetic susceptibility of the twinned sample which determines T_N. (c) and (d) The same as (a) and (b), respectively, but measured on the annealed FeTe single crystal. R_a (dashed curve) and R_b (dash-dotted curve) present the in-plane resistivity along the a'_O and b'_O directions with the uniaxial pressure for detwinning. R_{twin} (thin solid curve) is measured on the same sample when the pressure is not applied; thus it corresponds to the resistivity of the twinned crystal. Except those in the inset in (a), all the data were measured while warming the sample.

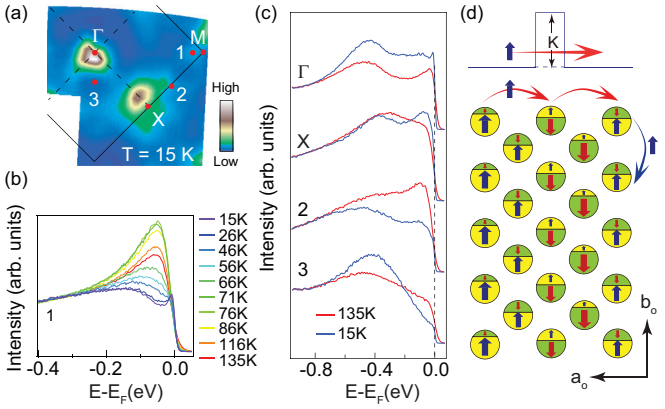

FIG. 3. (Color online) (a) Photoemission intensity distribution integrated over the energy window of $[E_F - 15\ \text{meV}, E_F + 15\ \text{meV}]$ for $Fe_{1.06}Te$ measured at 15 K. (b) Detailed temperature dependence of photoemission spectrum at momentum position 1 as marked in (a). (c) Temperature dependence of photoemission spectra at various momenta as marked in (a). (d) A schematic local picture of the bicollinear antiferromagnetic order in FeTe, where the arrows represent spins and the size of the arrows and the area that they occupy represent their population and size of the moment. Two hopping routes are demonstrated. When an up-spin electron hops along the AFM direction, it feels an additional potential K on the site with the localized moment pointing down. On the other hand, it moves freely in the FM direction.

Our early angle-resolved photoemission spectroscopy (ARPES) measurements[34] have illustrated the polaronic nature of FeTe. As shown in Fig. 3(a) for a twinned $Fe_{1.06}Te$ sample, the photoemission intensity around E_F is distributed as large patches over a broad momentum region, and the Fermi surface is poorly defined. In the high-temperature paramagnetic state, the photoemission spectrum is broad, and the single-particle excitation spectral function is overwhelmed by incoherent spectral weight [Fig. 3(b)], while a small but sharp quasiparticle peak emerges in the BCAF state. The incoherent spectral weight is responsible for the semiconducting behavior of the resistivity at high temperatures, and the small but coherent quasiparticle gives the metallic behavior below T_N. Figure 3(c) compares several typical spectra in the paramagnetic state and the BCAF state at various momenta in the Brillouin zone, which illustrates that the incoherent spectral weight is relocated over a large momentum and energy phase space across the BCAF transition. In general, it was found that the spectral weight is suppressed in the $[E_F - 0.4\ \text{eV}, E_F]$ region and enhanced in the $[E_F - 0.7\ \text{eV}, E_F - 0.2\ \text{eV}]$ region, which would significantly save the electronic energy and thus is sufficient to drive the phase transition.[34] These distinct electronic properties show that FeTe possesses the most localized and polaronic characteristics among all the iron-based compounds, and consistently, it has a large moment of $\sim 2\mu_B$ per Fe site, as observed in neutron-scattering experiments.[5] Therefore FeTe could be better understood from a localized picture as sketched in Fig. 3(d) and elaborated in the caption.[35] In this picture, the Hund's rule coupling between the itinerant electron (the small quasiparticle weight in the single-particle excitation spectrum, with spin 1/2) and the localized moment S would enforce an additional barrier K (proportional to $J_H S$) for the electrons hopping along the AFM direction, whereas those hopping along the FM direction are free of such a barrier [see Fig. 3(d)]. This naturally explains the observed resistivity anisotropy of FeTe.

From the electronic structure perspective, the distinct resistivity anisotropies in various iron pnictides and FeTe are the manifestation of the same physics in different regimes. For clarity, one could distinguish S as the "local moment" in iron pnictides and as the "localized moment" in FeTe. Iron pnictides are in the weak interaction or itinerant regime. The local moment there is the net moment due to the population difference between the majority and minority bands projected onto a particular site, which can be obtained by integrating the spin-dependent Bloch wave functions around a certain site in the itinerant picture. The finite local moments interact with an itinerant band through the Hund's rule coupling J_H and shift the energy of the parallel and antiparallel spins differently. Thus it causes remarkable electronic structure reconstruction observed by ARPES which was proposed to drive the CAF phase transitions.[19,36,37] This might contribute to the resistivity anisotropy observed in iron pnictides, although impurity scattering and orbital ordering should also be taken into account. On the other hand, FeTe is in the strong interaction or localized regime, where most of the electrons can be considered localized, and there is just a very small coherent quasiparticle weight. The itinerant electron interacts with the localized moment through Hund's rule coupling and feels an additional barrier K when hopping along the AFM direction. Therefore the resistivity in the AFM direction in FeTe is

larger than that in the FM direction. Theoretically, both the localized regime as in FeTe and the itinerant regime as in iron pnictides were unified by a recent dynamical mean-field theory plus density functional theory (DMFT + DFT) calculation that considers the Hund's rule coupling the most important local correlation.[38,39] The band structure reconstruction was reproduced, although it was not exactly like the experiment, and saving electronic energy through J_H is found to be the dominating force behind the nematic phase transitions. Moreover, the J_H effects are found to be outstanding for FeTe among various iron-based compounds. On a similar footing, a model containing both the itinerant electrons and local moments was proposed to unify the magnetic ground states in both the iron pnictides and FeTe.[35] Besides the various exchange interactions among neighboring sites,[33,40] it was proposed that the decisive parameter for magnetic order is the energy barrier K for the electron hopping between the antiparallel sites as depicted in Fig. 3(d), which is determined by the Hund's rule coupling energy. Based on these theories and our electronic structure and resistivity anisotropy measurements, FeTe could be considered Hund's metals.

Similar physics (multiband, polaronic electronic structure with strong Hund's rule coupling) has been observed before in the manganites.[41] Actually, a similar temperature dependence of resistivity is observed in $LaMnO_3$ doped with bivalent cations: above the Curie temperature, the resistivity behaves like a semiconductor, then a metallic conduction is observed in the ferromagnetic phase.[42] It has been well comprehended by the double-exchange model, where electrons hop freely when the local moments are ordered ferromagnetically. In the paramagnetic state, a random potential is enforced by J_H at sites whose moments are not parallel to the spin of the hopping electrons. Such randomness would cause localization and thus the insulating behavior. Therefore, just like the colossal magnetoresistivity, the resistivity anisotropy of FeTe is remarkable evidence of the crucial role of Hund's rule coupling.

III. CONCLUSION

To conclude, we report the temperature dependence of the resistivity anisotropy in a detwinned FeTe single crystal using the Montgomery method. The resistivity anisotropy of FeTe shows opposite behavior compared with that of the 122 series of iron pnictides; that is, the resistivity in the antiferromagnetic direction is larger than that in the ferromagnetic direction. The totally opposite resistivity behavior has the same physics as the colossal magnetoresistivity where Hund's rule coupling plays a very important role.

ACKNOWLEDGMENTS

We acknowledge the helpful discussions with Dr. Wei Ku, T. Liang, and S. Ishida. This work is supported in part by the National Science Foundation of China, the Ministry of Education of China, and the National Basic Research Program of China (973 Program) under Grants No. 2011CB921802, No. 2011CBA00112, and No. 2012CB921400.

*bpxie@fudan.edu.cn
†dlfeng@fudan.edu.cn

[1]Q. Huang, Y. Qiu, W. Bao, M. A. Green, J. W. Lynn, Y. C. Gasparovic, T. Wu, G. Wu, and X. H. Chen, Phys. Rev. Lett. **101**, 257003 (2008).
[2]D. K. Pratt, W. Tian, A. Kreyssig, J. L. Zarestky, S. Nandi, N. Ni, S. L. Bud'ko, P. C. Canfield, A. I. Goldman, and R. J. McQueeney, Phys. Rev. Lett. **103**, 087001 (2009).
[3]C. Lester, J.-H. Chu, J. G. Analytis, S. C. Capelli, A. S. Erickson, C. L. Condron, M. F. Toney, I. R. Fisher, and S. M. Hayden, Phys. Rev. B **79**, 144523 (2009).
[4]C. de la Cruz, Q. Huang, J. W. Lynn, J. Li, W. Ratcliff, II, J. L. Zarestky, H. A. Mook, G. F. Chen, J. L. Luo, N. L. Wang, and P. Dai, Nature (London) **453**, 899 (2008).
[5]S. Li, C. de la Cruz, Q. Huang, Y. Chen, J. W. Lynn, J. Hu, Y.-L. Huang, F.-C. Hsu, K.-W. Yeh, M.-K. Wu, and P. Dai, Phys. Rev. B **79**, 054503 (2009).
[6]J. Zhao, H. Cao, E. Bourret-Courchesne, D.-H. Lee, and R. J. Birgeneau, Phys. Rev. Lett. **109**, 267003 (2012).
[7]F. Chen, M. Xu, Q. Q. Ge, Y. Zhang, Z. R. Ye, L. X. Yang, J. Jiang, B. P. Xie, R. C. Che, M. Zhang, A. F. Wang, X. H. Chen, D. W. Shen, J. P. Hu, and D. L. Feng, Phys. Rev. X **1**, 021020 (2011).
[8]C. He, Y. Zhang, B. P. Xie, X. F. Wang, L. X. Yang, B. Zhou, F. Chen, M. Arita, K. Shimada, H. Namatame, M. Taniguchi, X. H. Chen, J. P. Hu, and D. L. Feng, Phys. Rev. Lett. **105**, 117002 (2010).
[9]C. Fang, H. Yao, W.-F. Tsai, J. Hu, and S. A. Kivelson, Phys. Rev. B **77**, 224509 (2008).
[10]J.-H. Chu, J. G. Analytis, K. De Greve, P. L. McMahon, Z. Islam, Y. Yamamoto, and I. R. Fisher, Science **329**, 824 (2010).
[11]S. Kasahara, H. J. Shi, K. Hashimoto, S. Tonegawa, Y. Mizukami, K. Sugimoto, T. Fukuda, T. Terashima, A. H. Nevidomskky, and Y. Mastuda, Nature (London) **486**, 382 (2012).
[12]T. Liang, M. Nakajima, K. Kihou, Y. Tomioka, T. Ito, C. H. Lee, H. Kito, A. Iyo, H. Eisaki, T. Kakeshita, and S. Uchida, J. Phys. Chem. Solids **72**, 418 (2011).
[13]S. Ishida, M. Nakajima, T. Liang, K. Kihou, C. H. Lee, A. Iyo, H. Eisaki, T. Kakeshita, Y. Tomioka, T. Ito, and S. Uchida, Phys. Rev. Lett. **110**, 207001 (2013).
[14]J. J. Ying, X. F. Wang, T. Wu, Z. J. Xiang, R. H. Liu, Y. J. Yan, A. F. Wang, M. Zhang, G. J. Ye, P. Cheng, J. P. Hu, and X. H. Chen, Phys. Rev. Lett. **107**, 067001 (2011).
[15]E. C. Blomberg, M. A. Tanatar, R. M. Fernandes, I. I. Mazin, B. Shen, H.-H. Wen, M. D. Johannes, J. Schmalian, and R. Prozorov, Nat. Commun. **4**, 1914 (2013).
[16]C.-C. Lee, W.-G. Yin, and W. Ku, Phys. Rev. Lett. **103**, 267001 (2009).
[17]R. M. Fernandes, A. V. Chubukov, J. Knolle, I. Eremin, and J. Schmalian, Phys. Rev. B **85**, 024534 (2012).
[18]E. P. Rosenthal, E. F. Andrade, C. J. Arguello, R. M. Fernandes, L. Y. Xing, X. C. Wang, C. Q. Jin, A. J. Millis, and A. N. Pasupathy, arXiv:1307.3526.

[19]Y. Zhang, C. He, Z. R. Ye, J. Jiang, F. Chen, M. Xu, Q. Q. Ge, B. P. Xie, J. Wei, M. Aeschlimann, X. Y. Cui, M. Shi, J. P. Hu, and D. L. Feng, Phys. Rev. B **85**, 085121 (2012).
[20]A. Jesche, F. Nitsche, S. Probst, Th. Doert, P. Muller, and M. Ruck, Phys. Rev. B **86**, 134511 (2012).
[21]M. B. Salamon and M. Jaime, Rev. Mod. Phys. **73**, 583 (2001).
[22]T. Taen, Y. Tsuchiya, Y. Nakajima, and T. Tamegai, Phys. Rev. B **80**, 092502 (2009).
[23]C. H. Dong, H. D. Wang, Z. J. Li, J. Chen, H. Q. Yuan, and M. H. Fang, Phys. Rev. B **84**, 224506 (2011).
[24]I. R. Fisher, L. Degiorgi, and Z. X. Shen, Rep. Prog. Phys. **74**, 124506 (2011).
[25]M. A. Tanatar, A. Kreyssig, S. Nandi, N. Ni, S. L. Bud'ko, P. C. Canfield, A. I. Goldman, and R. Prozorov, Phys. Rev. B **79**, 180508 (2009).
[26]S. Li, C. de la Cruz, Q. Huang, G. F. Chen, T.-L. Xia, J. L. Luo, N. L. Wang, and P. Dai, Phys. Rev. B **80**, 020504(R) (2009).
[27]H. C. Montgomery, J. Appl. Phys. **42**, 2971 (1971).
[28]B. F. Logan, S. O. Rice, and R. F. Wick, J. Appl. Phys. **42**, 2975 (1971).
[29]M. A. Tanatar, E. C. Blomberg, A. Kreyssig, M. G. Kim, N. Ni, A. Thaler, S. L. Bud'ko, P. C. Canfield, A. I. Goldman, I. I. Mazin, and R. Prozorov, Phys. Rev. B **81**, 184508 (2010).
[30]E. C. Blomberg, M. A. Tanatar, A. Kreyssig, N. Ni, A. Thaler, R. Hu, S. L. Bud'ko, P. C. Canfield, A. I. Goldman, and R. Prozorov, Phys. Rev. B **83**, 134505 (2011).
[31]M. H. Fang, H. M. Pham, B. Qian, T. J. Liu, E. K. Vehstedt, Y. Liu, L. Spinu, and Z. Q. Mao, Phys. Rev. B **78**, 224503 (2008).
[32]G. F. Chen, Z. G. Chen, J. Dong, W. Z. Hu, G. Li, X. D. Zhang, P. Zheng, J. L. Luo, and N. L. Wang, Phys. Rev. B **79**, 140509(R) (2009).
[33]W. Bao, Y. Qiu, Q. Huang, M. A. Green, P. Zajdel, M. R. Fitzsimmons, M. Zhernenkov, S. Chang, M. Fang, B. Qian, E. K. Vehstedt, J. Yang, H. M. Pham, L. Spinu, and Z. Q. Mao, Phys. Rev. Lett. **102**, 247001 (2009).
[34]Y. Zhang, F. Chen, C. He, L. X. Yang, B. P. Xie, Y. L. Xie, X. H. Chen, M. Fang, M. Arita, K. Shimada, H. Namatame, M. Taniguchi, J. P. Hu, and D. L. Feng, Phys. Rev. B **82**, 165113 (2010).
[35]W.-G. Yin, C.-C. Lee, and W. Ku, Phys. Rev. Lett. **105**, 107004 (2010).
[36]M. Yi, D. Lu, J.-H. Chu, J. G. Analytis, A. P. Sorini, A. F. Kemper, B. Moritz, S.-K. Mo, R. G. Moore, M. Hashimoto, W.-S. Lee, Z. Hussain, T. P. Devereaux, I. R. Fisher, and Z.-X. Shen, Proc. Natl. Acad. Sci. USA **108**, 6878 (2011).
[37]M. Yi, D. H. Lu, R. G. Moore, K. Kihou, C-H. Lee, A. Iyo, H. Eisaki, T. Yoshida, A. Fujimori, and Z.-X. Shen, New J. Phys. **14**, 073019 (2012).
[38]Z. P. Yin, K. Haule, and G. Kotliar, Nat. Phys. **7**, 294 (2011).
[39]Z. P. Yin, K. Haule, and G. Kotliar, Nat. Mater. **10**, 932 (2011).
[40]F. Ma, W. Ji, J. Hu, Z.-Y. Lu, and T. Xiang, Phys. Rev. Lett. **102**, 177003 (2009).
[41]N. Mannella, W. L. Yang, X. J. Zhou, H. Zheng, J. F. Mitchell, J. Zaanen, T. P. Devereaux, N. Nagaosa, Z. Hussain, and Z.-X. Shen, Nature (London) **438**, 474 (2005).
[42]A. Urushibara, Y. Moritomo, T. Arima, A. Asamitsu, G. Kido, and Y. Tokura, Phys. Rev. B **51**, 14103 (1995).